

Article

Comparison of the Lifshitz Theory Using the Nonconventional Fit of Response Functions with Precise Measurements of the Casimir Force

Galina L. Klimchitskaya ^{1,2}  and Vladimir M. Mostepanenko ^{1,2,3,*} 

¹ Central Astronomical Observatory at Pulkovo of the Russian Academy of Sciences, 196140 Saint Petersburg, Russia; g.klimchitskaya@gmail.com

² Peter the Great Saint Petersburg Polytechnic University, 195251 Saint Petersburg, Russia

³ Kazan Federal University, 420008 Kazan, Russia

* Correspondence: vmostepa@gmail.com

Abstract: It is known that the fundamental Lifshitz theory, which is based on the first principles of thermal quantum field theory, experiences difficulties when compared with precise measurements of the Casimir force. We analyzed the nonconventional fit of the response functions of many materials along the imaginary frequency axis to the empirical model of “modified” oscillators, which was recently proposed in the literature. According to our results, this model is unacceptable because at high frequencies it leads to the asymptotic behavior of the response functions, which is in contradiction with that following from the fundamental physical principles. We calculated the Casimir interaction in the configurations of several precise experiments using the Lifshitz theory and the response functions to the quantized electromagnetic field expressed in terms of modified oscillators and demonstrated that the obtained results are excluded by the measurement data. This invalidated a claim made in the literature that the Casimir–van der Waals forces calculated using these response functions are in remarkable agreement with the experimental values. Possible reasons for a disagreement between experiment and theory are discussed, and the way to improve the situation is indicated.

Keywords: Casimir interaction; response functions to the electromagnetic field; Lorentz oscillators; precise measurements of the Casimir force

Citation: Klimchitskaya, G.L.; Mostepanenko, V.M. Comparison of the Lifshitz Theory Using the Nonconventional Fit of Response Functions with Precise Measurements of the Casimir Force. *Symmetry* **2023**, *15*, 1011.

<https://doi.org/10.3390/sym15051011>

Academic Editor: Vladimir Dobrev

Received: 18 April 2023

Accepted: 28 April 2023

Published: 1 May 2023

Publisher’s Note: MDPI stays neutral with regard to jurisdictional claims in published maps and institutional affiliations.

Copyright: © 2023 by the authors. Submitted to *Symmetry* for possible open access publication under the terms and conditions of the Creative Commons Attribution (CC BY) license (<https://creativecommons.org/licenses/by/4.0/>).

1. Introduction

The physical nature of the Casimir (van der Waals in the nonrelativistic limit) forces determined by the zero-point and thermal fluctuations of the quantized electromagnetic field is widely covered in the literature (see the monographs [1–9] and the references therein). The fundamental theoretical description of these forces, which is based on thermal quantum field theory in the Matsubara formulation, was developed by E. M. Lifshitz [10,11]. It expresses the force value as a functional of the frequency-dependent response functions (dielectric permittivities) of the interacting bodies defined along the imaginary frequency axis. In the last few years, many experiments on measuring the Casimir–van der Waals force were performed, and their results were compared with theory (see the reviews [12–15]). For symmetric configurations (e.g., for two parallel plates or a sphere above a plate), the Casimir force acts perpendicular to the surfaces. If, however, the rotational symmetry is violated (e.g., for the plates covered with longitudinal coaxial corrugations), the lateral Casimir force may arise as well [8].

Currently, the Casimir–van der Waals forces are not only actively investigated in elementary particle physics, gravitation, cosmology, fundamental atomic, molecular, and condensed matter physics [1–9], but find application in micromechanics, microelectronics and nanoelectronics including organic electronics, various sensors, microswitches, analog integrated circuits, analog-to-digital and thermoelectric converters, etc. (see, e.g., [16–33]). Therefore, the possibility to reliably predict the force value on the basis of the fundamental Lifshitz theory is of the utmost importance. This, however, turned out to be a challenge. The point is that, to perform reliable computations using the Lifshitz theory, one needs to have at hand the response functions of the interacting bodies to the quantized electromagnetic field over rather wide frequency regions. Even when this information seems to be available, it happens that the computational results are in conflict with the measurement data [8,12,15,34,35].

Recently [36], the “self-consistent” (by the authors’ terminology) response functions for 55 materials over the full region of imaginary frequencies necessary for the calculation of Casimir–van der Waals forces were determined including common metals, organic and inorganic semiconductors, and insulators. According to [36], the Casimir–van der Waals forces calculated using these response functions “are in remarkable agreement with the experimental values reported over the span of the past half-century.”

The imaginary parts of the response functions of materials studied in [36] were compiled from the measured complex indices of refraction in different experiments. Thereafter, the response functions along the imaginary frequency axis have been obtained using the principle of causality expressed in the form of the Kramers–Kronig relations, which is the generally recognized way of calculations [6–9,12–15]. However, the article [36] claimed that the obtained response functions along the imaginary frequency axis are better fit not to the conventional Lorentz oscillators [5,8,37–39], but to the model of nonconventional “modified” oscillators. The latter model predicts that at high frequencies ω the response functions approach unity within the term decreasing as $\omega^{-\alpha}$, where $0 < \alpha < 2$, in place of the standard term decreasing as ω^{-2} .

In this paper, we call the reader’s attention to the fact that the high-frequency behavior of the response functions suggested by the model of modified oscillators is in contradiction with fundamental physical principles. Using the data of the most precise experiments on measuring the Casimir interaction between metallic surfaces, we also show that theoretical predictions of the Lifshitz theory found with the model of modified oscillators are excluded at a high confidence level. Thus, the conclusion of [36] about a remarkable agreement between the theoretical results obtained using the “self-consistent” response functions and the experimental values is invalidated. The reason why an unjustified conclusion has been made is that [36] did not use the data of the most precise experiments when performing the theory–experiment comparison.

The paper is organized as follows. In Section 2, we confront the representations of response functions using the models of the Lorentz and modified oscillators. Section 3 contains a comparison of the theoretical results computed with the model of modified oscillators and the measured Casimir interaction between Au surfaces. In Section 4, a similar comparison is performed with the measured Casimir interaction between magnetic (Ni) surfaces. In Section 5, the reader will find our discussion of possible reasons for a disagreement between experiment and theory, and in Section 6 we give our conclusions, where a line of attack on the problem is directed.

2. Representation of the Dielectric Functions Using the Lorentz Oscillators and the Nonconventional Modified Oscillators

It is common knowledge that a reasonably accurate and yet simple representation for the response functions of different insulator materials to the electromagnetic field is given

by the sum of the appropriate number of Lorentz oscillators describing the bound (core) electrons [5,8,37–39]:

$$\varepsilon_I(\omega) = 1 + \sum_{j=1}^K \frac{g_j}{1 - \left(\frac{\omega}{\omega_j}\right)^2 - i\frac{\gamma_j\omega}{\omega_j^2}}, \quad (1)$$

where K is the number of oscillators, $\omega_j \neq 0$ are the oscillator frequencies, γ_j are the relaxation parameters, and g_j are proportional to the oscillator strengths. The representation (1) works well for the materials whose molecules do not possess intrinsic dipole moments. For the polar dielectrics, the molecules of which possess intrinsic dipole moments oriented in an electromagnetic field, one more (Debye) term should be added on the right-hand side of (1).

If the boundary material is metallic, there is also an additional oscillator term in (1) with zero oscillator frequency, $\omega_0 = 0$, describing the conduction (free) electrons. As a result, the response functions of metallic materials take the form:

$$\varepsilon_M(\omega) = -\frac{g_0}{\omega(\omega + i\gamma_0)} + \varepsilon_I(\omega), \quad (2)$$

which is known as the dielectric permittivity of the Drude model. In this case, g_0 has the meaning of the plasma frequency squared, $g_0 = \omega_p^2$.

The response functions (1) and (2) satisfy the principle of causality, which is expressed mathematically in the form of the Kramers–Kronig relations connecting their imaginary and real parts [40]. Substituting $\omega = i\zeta$, one obtains the response functions of insulators and metals defined along the imaginary frequency axis:

$$\begin{aligned} \varepsilon_I(i\zeta) &= 1 + \sum_{j=1}^K \frac{g_j}{1 + \left(\frac{\zeta}{\omega_j}\right)^2 + \frac{\gamma_j\zeta}{\omega_j^2}}, \\ \varepsilon_M(i\zeta) &= \frac{\omega_p^2}{\zeta(\zeta + \gamma_0)} + \varepsilon_I(i\zeta). \end{aligned} \quad (3)$$

Note that the same expressions result from $\text{Im}\varepsilon_{I,M}$ by using the dispersion relation [40]:

$$\varepsilon_{I,M}(i\zeta) = 1 + \frac{2}{\pi} \int_0^\infty \frac{\omega \text{Im}\varepsilon_{I,M}(\omega)}{\omega^2 + \zeta^2} d\omega. \quad (4)$$

It should be pointed out that at short separations between the interacting bodies the major contribution to the Lifshitz formula for the Casimir–van der Waals force is given by the large $\zeta \gg \gamma_j$. Because of this, (3) can be rewritten in a simpler form:

$$\begin{aligned} \varepsilon_I(i\zeta) &\approx 1 + \sum_{j=1}^K \frac{g_j}{1 + \left(\frac{\zeta}{\omega_j}\right)^2}, \\ \varepsilon_M(i\zeta) &\approx \varepsilon_I(i\zeta), \end{aligned} \quad (5)$$

which is referred to as the Ninham–Parsegian representation [37,38]. Thus, at short separations, the force is mostly determined by the core (bound) electrons.

As to the case of large separations, where the major contribution to the force is given by the zero Matsubara frequency (see the next section), one arrives at

$$\begin{aligned}\varepsilon_I(i\tilde{\zeta}) &\approx \varepsilon_I(0) = 1 + \sum_{j=1}^K g_j, \\ \varepsilon_M(i\tilde{\zeta}) &\approx \frac{\omega_p^2}{\tilde{\zeta}(\tilde{\zeta} + \gamma_0)}.\end{aligned}\quad (6)$$

This means that for metals the force value is determined by the free (conduction) electrons.

For materials that exhibit an electronic polarization only (for Si, for instance), the sum in (5) may be replaced by one effective oscillator term with a frequency ω_{UV} belonging to the ultraviolet region. As for materials that also exhibit an ionic polarization (SiO_2 , for instance), their response function may be presented as a sum of one effective oscillator with a frequency ω_{UV} and another one whose frequency ω_{IR} belongs to the infrared region:

$$\varepsilon_I(i\tilde{\zeta}) = 1 + \frac{g_{UV}}{1 + \left(\frac{\tilde{\zeta}}{\omega_{UV}}\right)^2} + \frac{g_{IR}}{1 + \left(\frac{\tilde{\zeta}}{\omega_{IR}}\right)^2}.\quad (7)$$

Equations (3), (5), and (7) have been extensively used in the literature (see, e.g., [39, 41]) to fit the measured data for the response functions of many materials. The obtained expressions were extensively applied to compute the Casimir–van der Waals forces (see the lists of references in the monographs [2–9]).

At high frequencies, (3), (5), and (7) predict the following similar asymptotic behavior for the response functions of both insulating and metallic materials:

$$\varepsilon(\omega) - 1 \sim \frac{1}{\omega^2}, \quad \varepsilon(i\tilde{\zeta}) - 1 \sim \frac{1}{\tilde{\zeta}^2}.\quad (8)$$

According to [36], however, this prediction is incorrect. In support of this claim, some optical data for water, SiO_2 , and LiF were collected, which seemingly yielded the electronic contribution to the dielectric functions along the imaginary frequency axis obeying at high frequencies the law [36]:

$$\varepsilon_{el}(i\tilde{\zeta}) - 1 \sim \frac{1}{\tilde{\zeta}^\alpha},\quad (9)$$

where $0 < \alpha < 2$ in place of (8).

On this basis, Reference [36] argued that the electronic contribution to the response function commonly described by the first two terms on the right-hand side of (7) can be modified to an empirical relationship:

$$\varepsilon_{el}(i\tilde{\zeta}) = 1 + \frac{g_{UV}}{1 + \left(\frac{\tilde{\zeta}}{\omega_{UV}}\right)^\alpha}.\quad (10)$$

It is easily seen, however, that (9) and, thus, (10) are invalid. As explained in [40], if the field frequency ω is much larger compared to the frequencies of almost all atomic electrons, the latter can be considered as free particles not interacting between themselves and with atomic nuclei. The velocities of electrons in atoms v are small compared to the speed of light c . Because of this, the distances $2\pi v/\omega$ traveled by electrons during a period of the electromagnetic wave are small in comparison to the wavelength $2\pi c/\omega$.

As a consequence, when finding the velocity of an electron in the electromagnetic field of a wave, the latter can be considered as spatially homogeneous. Under these conditions, solving the equation of motion and calculating the polarization of the material by summing over all electrons in the unit volume, one arrives at [40]

$$\varepsilon(\omega) = 1 - \frac{4\pi Ne^2}{m_e \omega^2}, \quad \varepsilon(i\zeta) = 1 + \frac{4\pi Ne^2}{m_e \zeta^2}, \quad (11)$$

where m_e and e are the mass and charge of an electron and N is the number of electrons in all atoms of the unit of volume of a material.

We underline that (11) is a universal result following from the basic physical principles, and it is valid for the response functions of any material: insulator, metal, or semiconductor. For light elements, the application region of (11) starts from the far ultraviolet (6 eV–10 eV) and for heavier elements from the X-ray frequencies (100 eV–100 keV) [40]. Thus, if some used sets of the measured optical data (often taken from different sources) lead to the response function $\varepsilon(i\zeta)$, which does not satisfy (11) at sufficiently high frequencies, one should cast doubt on these data.

3. Comparison Between Measured and Calculated Casimir–van der Waals Forces Using the Nonconventional Fit to the Modified Oscillators for Gold Test Bodies

According to [36], the “self-consistent” response function of Au presented by (2) using the fit to a modified oscillator is given by (see the Supplemental Materials in [42] to [36])

$$\varepsilon_{\text{Au}}(i\zeta) = 1 + \frac{(9.1)^2}{\zeta(\zeta + 0.06)} + \frac{6.5}{1 + \left(\frac{\zeta}{5.9}\right)^{1.42}}, \quad (12)$$

where $\omega_p = 9.1$ eV, $\gamma_0 = 0.06$ eV, $g_{\text{UV}} = 6.5$, $\omega_{\text{UV}} = 5.9$ eV, and $\alpha = 1.42$ (the frequency ζ is measured in eV).

Reference [36] claimed that the theoretical Casimir–van der Waals forces calculated using the “self-consistent” response functions in the framework of the Lifshitz theory match remarkably well with the experimentally measured forces. It is well known that the most precise measurements of the Casimir–van der Waals forces were performed between an Au-coated sphere and an Au-coated plate separated with a vacuum gap [8,12]. In Figure 5 of [36], the theory–experiment comparison of this kind was presented, however, only for two and not the most precise experiments [43,44] performed long ago.

Thus, in the experiment [43], the Casimir force was measured between the Au-coated surfaces of a sphere and a plate by means of an atomic force microscope operated in static mode. Here, we calculated the Casimir force in the experimental configuration of [43] using the Lifshitz theory and the “self-consistent” response function (12) with the properly accounted-for effect of surface roughness as described in [45,46].

The Casimir force acting between a sphere of radius R spaced at a distance $a \ll R$ above a plate at temperature T in thermal equilibrium with the environment is expressed by the following Lifshitz formula [8,12]:

$$F(a) = k_B T R \sum_{l=0}^{\infty}{}' \int_0^{\infty} k_{\perp} dk_{\perp} \sum_{\alpha} \ln \left[1 - r_{\alpha}^2(i\zeta_l, k_{\perp}) e^{-2aq_l} \right]. \quad (13)$$

Here, k_B is the Boltzmann constant, k_{\perp} is the magnitude of the wave vector component along the plate, $\zeta_l = 2\pi k_B T l / \hbar$ are the Matsubara frequencies with $l = 0, 1, 2, \dots$, the prime on the first summation sign divides the term with $l = 0$ by 2, and the summation in α is over two independent polarizations of the electromagnetic field, transverse magnetic (α

= TM) and transverse electric ($\alpha = \text{TE}$). The reflection coefficients calculated at the pure imaginary Matsubara frequencies are given by

$$r_{\text{TM}}(i\zeta_l, k_{\perp}) = \frac{\varepsilon_l q_l - k_l}{\varepsilon_l q_l + k_l}, \quad r_{\text{TE}}(i\zeta_l, k_{\perp}) = \frac{\mu_l q_l - k_l}{\mu_l q_l + k_l}, \quad (14)$$

where $\varepsilon_l = \varepsilon(i\zeta_l)$, the magnetic permeability $\mu_l = \mu(i\zeta_l)$ describes the response of materials to the magnetic field (for Au $\mu(\omega) = 1$), and the following notations are introduced:

$$q_l = \left(k_{\perp}^2 + \frac{\zeta_l^2}{c^2} \right)^{1/2}, \quad k_l = \left[k_{\perp}^2 + \varepsilon_l \mu_l \frac{\zeta_l^2}{c^2} \right]^{1/2}. \quad (15)$$

Equation (13) is written in the proximity force approximation [8,12]. The exact theory using the scattering approach demonstrates that, at short separations $a \ll R$, the corrections to (13) do not exceed the fraction of a/R [47–54]. These corrections are negligibly small in the configurations of precise experiments on measuring the Casimir force [8,12,34,35].

The theoretical results taking into account the surface roughness are obtained from (13) by the geometrical averaging over the measured roughness profiles of the plate and sphere surfaces [6,12]:

$$F_R(a) = \sum_{i,k} v_i^{(1)} v_k^{(2)} F(a + H_0^{(1)} + H_0^{(2)} - h_i^{(1)} - h_k^{(2)}), \quad (16)$$

where $v_i^{(1)}(v_k^{(2)})$ are the fractions of the plate (sphere) areas with heights $h_i^{(1)}(h_k^{(2)})$. Here, $H_0^{(1,2)}$ are the zero levels relative to which the mean values of the roughness profiles on both bodies are zero. It was shown [8,12,34] that at short separations, where the effect of surface roughness should be taken into account, the more fundamental analysis based on the scattering approach [55] leads to approximately the same results as the method of geometrical averaging.

The computational results obtained using (12), (13), and (16) are shown in Figure 1 by the black band, whose width is determined by the theoretical errors calculated at the 95% confidence level. In the same figure, the measurement data are indicated as crosses, whose arms show the experimental errors in measuring the absolute separations and forces, which were also determined at the 95% confidence level.

As is seen in Figure 1, the agreement between experiment and theory cannot be called remarkably good because some of the crosses do not even touch the theoretical band. Reference [36] recognized the presence of some deviations between the theoretical results computed using the modified oscillators and the measurement data, especially at short separations, but attributes them to the probable role of surface roughness and to the sub-nanometer errors in the estimation of the separation distances. However, in the theory–experiment comparison presented here in Figure 1, both of these effects were addressed quantitatively and taken into account.

The more precise modern experiments on measuring the Casimir interaction demonstrated the total discrepancy between the theoretical predictions using the dielectric functions of [36] and the measurement data. In Figure 2a–f, the experimental data of [56,57] for determining the effective Casimir pressure $P_R(a)$ between the Au-coated surfaces of two parallel plates by means of a micromechanical torsional oscillator are shown as crosses over six different separation intervals. The theoretical bands are computed here using the

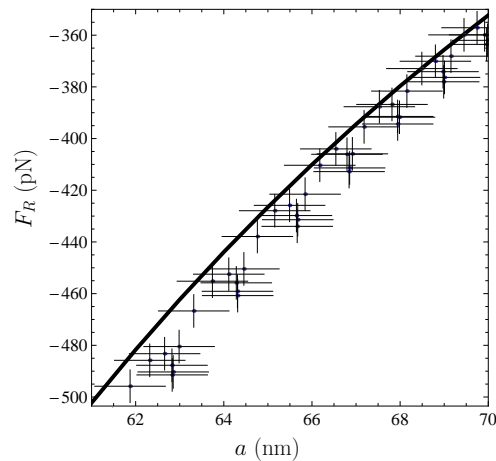


Figure 1. Predictions of the Lifshitz theory for the Casimir force between the Au surfaces of a sphere and a plate obtained using the modified oscillator in the experimental configuration of [43] are shown by the black band. The measurement data of [43,45] are indicated as crosses, whose arms are determined at the 95% confidence level.

dielectric function (12) with the account of the surface roughness by the Lifshitz formula [8,12]:

$$P_R(a) = -\frac{1}{2\pi R} \frac{dF_R(a)}{da}. \quad (17)$$

Both the arms of the crosses and the widths of the bands are again found at the 95% confidence level (see [56,57] for the details of the computations).

As is seen in Figure 2, the theoretical predictions found by using the “self-consistent” dielectric functions of Au (12) are excluded by the measurement data at the 95% confidence level over the entire measurement range.

In one more precise experiment, the gradient of the Casimir force $dF_R(a)/da$ acting between the Au-coated surfaces of a sphere and a plate was measured by means of a dynamic atomic force microscope [58]. The experimental data measured in this experiment are shown as crosses over the three separation intervals in Figure 3a–c.

The theoretical bands are again computed with the account of the surface roughness by using (13), (16), and the “self-consistent” response function (12). In this case, all errors were determined at the 67% confidence level. From Figure 3, one can conclude that the theoretical predictions obtained using the response function (12) are excluded by the measurement data of [58].

We note that the data of the most precise experiments [56–58], measuring the Casimir interaction between two Au surfaces separated by a vacuum gap, were not considered and compared with the suggested approach of [36] using a nonconventional fit of the response functions to the modified oscillators. As a result, an invalid conclusion has been made that the Casimir–van der Waals interaction computed using these response functions agree remarkably well with the experimental results.

4. Comparison Between Measured and Calculated Casimir–van der Waals Forces Using the Nonconventional Fit to the Modified Oscillators for Nickel Test Bodies

Measurements of the Casimir interaction for the test bodies made of a magnetic metal Ni play an especially important role in Casimir physics because the magnetic properties of a material, along with the dielectric ones, produce a pronounced impact on the force value.

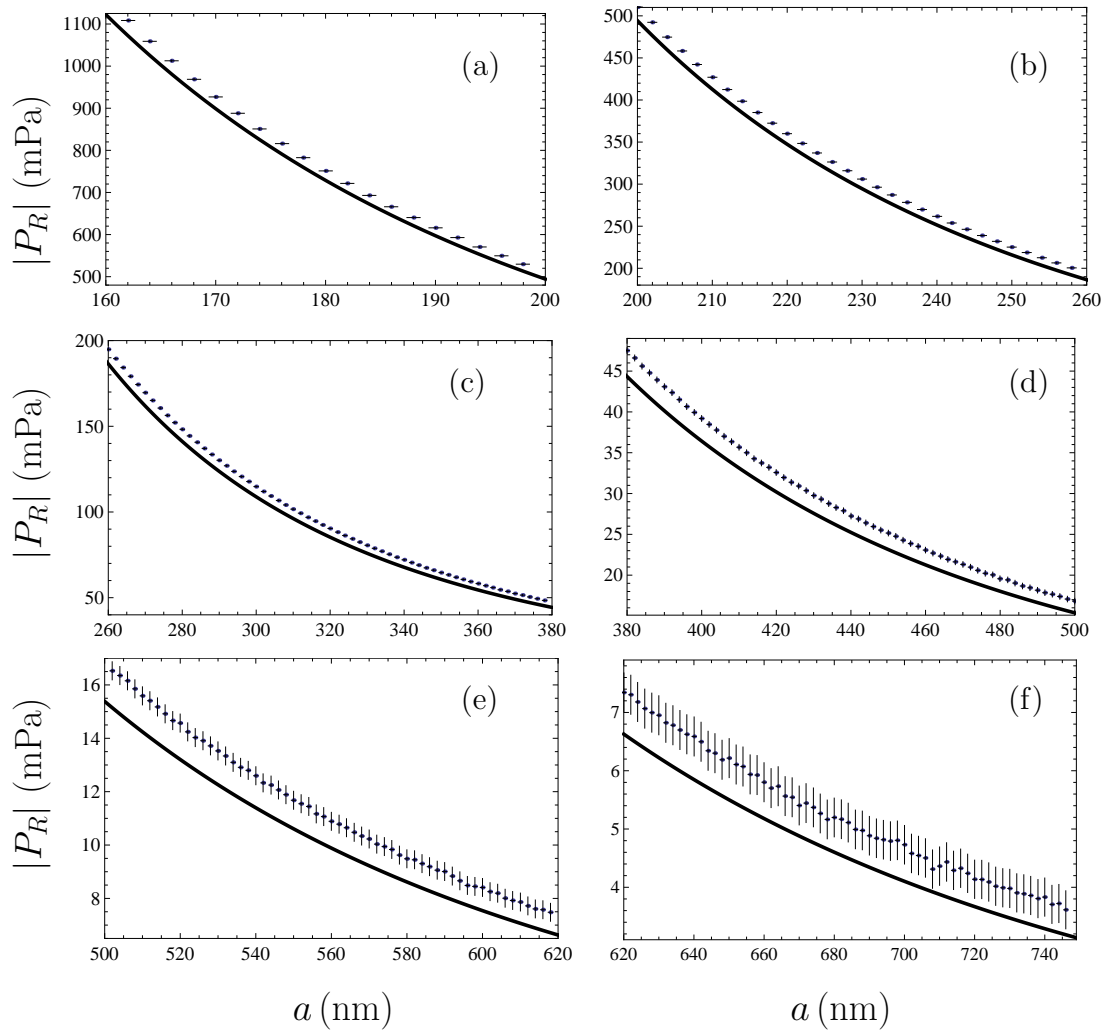


Figure 2. Predictions of the Lifshitz theory for the effective Casimir pressure between two Au plates obtained using the modified oscillator in the experimental configuration of [46,47] are shown by the black bands over different separation intervals. The measurement data of [46,47] are indicated as crosses, whose arms are determined at the 95% confidence level. In all subfigures a-f, the theoretical predictions obtained using (12) are excluded by the measurement data.

The gradient of the Casimir force between the Ni-coated surfaces of a sphere and a plate separated by a vacuum gap was measured in [59,60] by means of a dynamic atomic force microscope.

Here, we compared the obtained measurement data with the theoretical predictions of the Lifshitz theory found using the “self-consistent” response function of Ni presented in the form of a modified oscillator in [36,42]:

$$\varepsilon_{\text{Ni}}(i\xi) = 1 + \frac{(4.33)^2}{\xi(\xi + 0.0195)} + \frac{115}{1 + \left(\frac{\xi}{0.61}\right)^{1.35}}, \quad (18)$$

where $\omega_p = 4.33$ eV, $\gamma_0 = 0.0195$ eV, $g_{\text{UV}} = 115$, $\omega_{\text{UV}} = 0.61$ eV, and $\alpha = 1.35$.

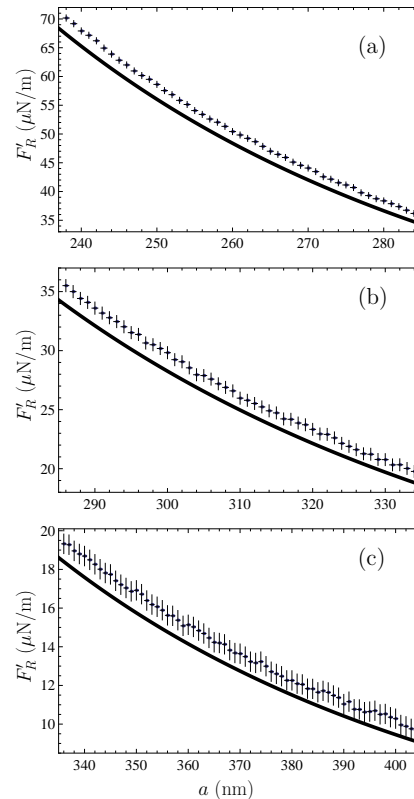


Figure 3. Predictions of the Lifshitz theory for the gradient of the Casimir force between the Au surfaces of a sphere and a plate obtained using the modified oscillator in the experimental configuration of [48] are shown by the black bands over different separation intervals. The measurement data of [48] are indicated as crosses, whose arms are determined at the 67% confidence level. In all subfigures a-c, the theoretical predictions obtained using (12) are excluded by the measurement data.

The theoretical band for the gradient of the Casimir force calculated using (13) and (18) with the account of the surface roughness is shown in Figure 4a,b in two different separation intervals. These calculations take into account the static magnetic permeability of Ni, $\mu_0(0) = 110$, entering the Lifshitz formula through the reflection coefficients (14) at zero Matsubara frequency [59,60]. Note that the magnetic properties of a material do not contribute to all Matsubara terms of (13) with $l \geq 1$ because $\mu(i\zeta)$ quickly drops to unity with increasing ζ [61]. The experimental data for the measured gradients are indicated as crosses. Here, we recalculated the arms of these crosses to the 95% confidence level (in the original publications, the errors were determined at the 67% confidence level).

As is seen in Figure 4, the theoretical predictions obtained using the nonconventional fit of the optical data to the modified oscillator (18) are excluded by the measurement data over the separation distances from 222 to 335 nm.

A comparison between Figure 4 and Figure 3 shows an important difference between the cases of magnetic (Ni) and nonmagnetic (Au) metals. From Figure 4, it is seen that for a magnetic metal the theoretically predicted force gradients are larger than the measured values, whereas for a nonmagnetic metal the measured force gradients are in excess of the computed results. This fact was used in [59,60] to underline the existence of a serious unresolved problem in the calculation of the Casimir–van der Waals forces. Although in

the experiments mentioned above a gap between the computed and observed values is of about a few percent, in measuring the differential Casimir forces the theoretical predictions of the Lifshitz theory differ from the measured values by up to a factor of 1000 [62]. This is a reason why the importance of the observed disagreement between experiment and theory should not be underestimated.

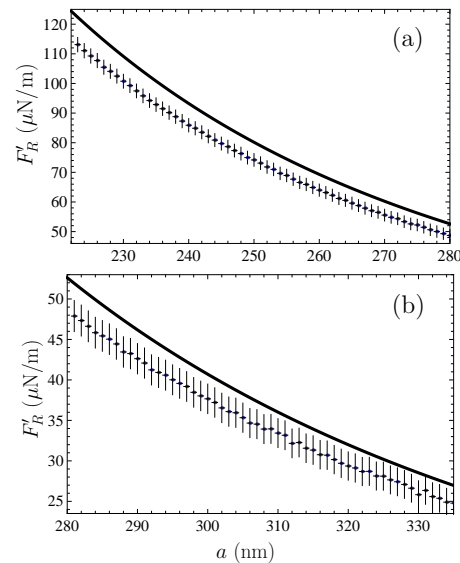


Figure 4. Predictions of the Lifshitz theory for the gradient of the Casimir force between the Ni surfaces of a sphere and a plate obtained using the modified oscillator in the experimental configuration of [49,50] are shown by the black bands over different separation intervals. The measurement data of [49,50] are indicated as crosses, whose arms are determined at the 95% confidence level. In both subfigures a,b, the theoretical predictions obtained using (18) are excluded by the measurement data.

5. Discussion

In the foregoing, we analyzed the recently proposed nonconventional fit of the response functions of a wide class of materials along the imaginary frequency axis to the so-called “modified” oscillators [36,42]. It was demonstrated that the mere form of the modified oscillator is unacceptable because it leads to an incorrect asymptotic behavior of the response functions at high frequencies, which is in contradiction with the fundamental physical principles. What is more, we calculated the Casimir–van der Waals interaction in the configurations of several precise experiments using the formalism of the modified oscillators and found that the obtained computational results are excluded by the measurement data.

The opposite result obtained in [36] is explained by the fact that the authors did not consider the most precise experiments and presented the results of their comparison in the logarithmic scale, which does not allow an informative discrimination between different lines. Note also that [36] arrived at a misleading result that “In the case of metals,... the role of interband transitions on the magnitude of van der Waals–Casimir forces becomes crucial once the ratio of charge carriers to total electrons in the systems becomes small.” In fact, as outlined in Section 2, for a particular metal, the relative role of the core and conduction electrons depends on the separation distance between the test bodies made of this metal. At separations much smaller than a micrometer, the major contribution to the

Casimir–van der Waals force is given by the core (bound) electrons, whereas at separations in excess of several micrometers the force value is determined by the conduction electrons. Keeping in mind the wide application areas of the Casimir–van der Waals forces and the many publications using the dielectric functions of diverse materials in the computations, the above clarifications regarding [36] seem pertinent.

6. Conclusions

We conclude with a short remark on the general situation in the theory of Casimir–van der Waals forces. It has been long known that the standard description of free charge carriers by means of the Drude model leads to contradictions between experiment and theoretical Casimir forces even if the conventional fit of the optical data to the Lorentz oscillators is employed [8,12,14,15,56–60,62]. When using the standard sets of optical data from Palik’s handbook [63], the theory comes to an agreement with the measurement results if the conduction electrons are described by the dissipationless plasma model [8,12,14,15,56–60,62]. This fact, however, has no commonly accepted theoretical explanation (note that with the values of the plasma frequency found in [36] an agreement between experiment and theory is lacking regardless of what model is chosen for a description of conduction electrons). Similar problems arise for the Casimir force acting between insulator test bodies [8,12,64–67]. There is a possibility to deal with these problems using the so-called “weighted” Kramers–Kronig relations [68], which allow the mathematical derivation of the response function of a material outside the region where it is measured with sufficient precision. This method, however, relies on the known behavior at zero frequency, which is different for the Drude and plasma response functions.

It was hypothesized that the above problems derive from the fact that the Drude model is not applicable in the area of the low-frequency s-polarized evanescent waves, where it has no sufficient experimental confirmation [69,70]. An experiment was proposed allowing one to check this hypothesis [69,70]. The possible resolution of the problem might be found in the search for spatially nonlocal generalizations of the Drude model at low frequencies [71,72]. Several promising opportunities on this way are in sight.

Funding: The work of G.L.K. was partially funded by the Ministry of Science and Higher Education of the Russian Federation (“The World-Class Research Center: Advanced Digital Technologies”, Contract No. 075-15-2022-311 dated April 20, 2022). The research of V.M.M. was partially carried out in accordance with the Strategic Academic Leadership Program “Priority 2030” of the Kazan Federal University.

References

1. Mahanty, J.; Ninham, B.W. *Dispersion Forces*; Academic Press: London, UK, 1976.
2. Milonni, P.W. *The Quantum Vacuum. An Introduction to Quantum Electrodynamics*; Academic Press: San Diego, CA, USA, 1994.
3. Mostepanenko, V.M.; Trunov, N.N. *The Casimir Effect and Its Applications*; Clarendon Press: Oxford, UK, 1997.
4. Milton, K.A. *The Casimir Effect: Physical Manifestations of Zero-Point Energy*; World Scientific: Singapore, 2001.
5. Parsegian, V.A. *Van der Waals Forces: A Handbook for Biologists, Chemists, Engineers, and Physicists*; Cambridge University Press: Cambridge, UK, 2005.
6. Buhmann, S.Y. *Dispersion Forces*; Springer: Berlin, Germany, 2012; Volumes 1 and 2.
7. Langbein, D. *Theory of Van der Waals Attraction*; Springer: Berlin/Heidelberg, Germany, 2013.
8. Bordag, M.; Klimchitskaya, G.L.; Mohideen, U.; Mostepanenko, V.M. *Advances in the Casimir Effect*; Oxford University Press: Oxford, UK, 2015.
9. Sernelius, B.E. *Fundamentals of van der Waals and Casimir Interactions*; Springer: New York, NY, USA, 2018.
10. Lifshitz, E.M. The theory of molecular attractive forces between solids. *Zh. Eksp. Teor. Fiz.* **1955**, *29*, 94–110; Translated: *Sov. Phys. JETP* **1956**, *2*, 73–83.
11. Lifshitz, E.M.; Pitaevskii, L.P. *Statistical Physics*; Pt II; Pergamon: Oxford, UK, 1980.

12. Klimchitskaya, G.L.; Mohideen, U.; Mostepanenko, V.M. The Casimir force between real materials: Experiment and theory. *Rev. Mod. Phys.* **2009**, *81*, 1827–1885.
13. Rodrigues, A.W.; Capasso, F.; Johnson, S.G. The Casimir effect in microstructured geometries. *Nat. Photon.* **2011**, *5*, 211–221.
14. Klimchitskaya, G.L.; Mohideen, U.; Mostepanenko, V.M. Control of the Casimir force using semiconductor test bodies. *Int. J. Mod. Phys. B* **2011**, *25*, 171–230.
15. Woods, L.M.; Dalvit, D.A.R.; Tkatchenko, A.; Rodriguez-Lopez, P.; Rodriguez, A.W.; Podgornik, R. Materials perspective on Casimir and van der Waals interactions. *Rev. Mod. Phys.* **2016**, *88*, 045003.
16. Buks, E.; Roukes, M.L. Stiction, adhesion, and the Casimir effect in micromechanical systems. *Phys. Rev. B* **2001**, *63*, 033402.
17. Buks, E.; Roukes, M.L. Metastability and the Casimir effect in micromechanical systems. *Europhys. Lett.* **2001**, *54*, 220–226.
18. Chan, H.B.; Aksyuk, V.A.; Kleiman, R.N.; Bishop, D.J.; Capasso, F. Quantum mechanical actuation of microelectromechanical system by the Casimir effect. *Science* **2001**, *291*, 1941–1944.
19. Chan, H.B.; Aksyuk, V.A.; Kleiman, R.N.; Bishop, D.J.; Capasso, F. Nonlinear Micromechanical Casimir Oscillator. *Phys. Rev. Lett.* **2001**, *87*, 211801.
20. Barcenas, J.; Reyes, L.; Esquivel-Sirvent, R. Scaling of micro- and nanodevices actuated by the Casimir force. *Appl. Phys. Lett.* **2005**, *87*, 263106.
21. Palasantzas, G. Contact angle influence on the pull-in voltage of microswitches in the presence of capillary and quantum vacuum effects. *J. Appl. Phys.* **2007**, *101*, 053512.
22. Palasantzas, G. Pull-in voltage of microswitch rough plates in the presence of electromagnetic and acoustic Casimir forces. *J. Appl. Phys.* **2007**, *101*, 063548.
23. Esquivel-Sirvent, R.; Pérez-Pascual, R. Geometry and charge carrier induced stability in Casimir actuated nanodevices. *Eur. Phys. J. B* **2013**, *86*, 467.
24. Broer, W.; Palasantzas, G.; Knoester, G.; Svetovoy, V.B. Significance of the Casimir force and surface roughness for actuation dynamics of MEMS. *Phys. Rev. B* **2013**, *87*, 125413.
25. Sedighi, M.; Broer, W.; Palasantzas, G.; Kooi, B.J. Sensitivity of micromechanical actuation on amorphous to crystalline phase transformations under the influence of Casimir forces. *Phys. Rev. B* **2013**, *88*, 165423.
26. Zou, J.; Marcet, Z.; Rodriguez, A.W.; Reid, M.T.H.; McCauley, A.P.; Kravchenko, I.I.; Lu, T.; Bao, Y.; Johnson, S.G.; Chan, H.B. Casimir forces on a silicon micromechanical chip. *Nat. Commun.* **2013**, *4*, 1845.
27. Broer, W.; Waalkens, H.; Svetovoy, V.B.; Knoester, J.; Palasantzas, G. Nonlinear Actuation Dynamics of Driven Casimir Oscillators with Rough Surfaces. *Phys. Rev. Appl.* **2013**, *4*, 054016.
28. Liu, X.-F.; Li, Y.; Jing, H. Casimir switch: Steering optical transparency with vacuum forces. *Sci. Rep.* **2016**, *6*, 27102.
29. Inui, N. Optical switching of a graphene mechanical switch using the Casimir effect. *J. Appl. Phys.* **2017**, *122*, 104501.
30. Klimchitskaya, G.L.; Mostepanenko, V.M.; Petrov, V.M.; Tschudi, T. Demonstration of the Optical Chopper Driven by the Casimir Force. *Phys. Rev. Appl.* **2018**, *10*, 014010.
31. Panda, S.S.; Katz, H.E.; Tovar, J.D. Solid-state electrical applications of protein and peptide based nanomaterials. *Chem. Soc. Rev.* **2018**, *47*, 3640–3658.
32. Klimchitskaya, G.L.; Mostepanenko, V.M.; Velichko, E.N. Casimir pressure in peptide films on metallic substrates: Change of sign via graphene coating. *Phys. Rev. B* **2021**, *103*, 245421.
33. Klimchitskaya, G.L.; Mostepanenko, V.M.; Tsybin, O.Yu. Attractive and Repulsive Fluctuation Induced Pressure in Peptide Films Deposited on Semiconductor Substrates. *Symmetry* **2022**, *14*, 2196.
34. Mostepanenko, V.M. Casimir Puzzle and Conundrum: Discovery and Search for Resolution. *Universe* **2021**, *7*, 84.
35. Klimchitskaya, G.L.; Mostepanenko, V.M. Current status of the problem of thermal Casimir force. *Int. J. Mod. Phys. A* **2022**, *37*, 2241002.
36. Moazzami Gudarzi, M.; Aboutalebi, S.H. Self-consistent dielectric functions of materials: Toward accurate computation of Casimir–van der Waals forces. *Sci. Advances* **2021**, *7*, eabg2272.
37. Parsegian, V.A.; Ninham, B.W. Application of the Lifshitz theory to the calculation of van der Waals forces across thin lipid films. *Nature* **1969**, *224*, 1197–1198.
38. Ninham, B.W.; Parsegian, V.A. Van der Waals forces: Special characteristics in lipid-water systems and a general method of calculation based on the Lifshitz theory. *Biophys. J.* **1970**, *10*, 646–663.
39. Bergström, L. Hamaker constant of inorganic materials. *Adv. Coll. Interface Sci.* **1979**, *70*, 125–169.
40. Landau, L.D.; Lifshitz, E.M.; Pitaevskii, L.P. *Electrodynamics of Continuous Media*; Pergamon: Oxford, UK, 1984.
41. Hough, D.B.; White, L.H. The calculation of Hamaker constant from Lifshitz theory with application to wetting phenomena. *Adv. Coll. Interface Sci.* **1980**, *14*, 3–41.
42. Moazzami Gudarzi, M.; Aboutalebi, S.H. Supplementary materials to [36]. Available online: <http://advances.sciencemag.org/cgi/content/full> (accessed on 14 April 2023).
43. Harris, B.W.; Chen, F.; Mohideen, U. Precise measurement of the Casimir force using gold surfaces. *Phys. Rev. A* **2000**, *62*, 052109.

44. van Zwol, P.J.; Palasantzas, G.; De Hosson, J.Th.M. Influence of random roughness on the Casimir force at small separations. *Phys. Rev. B* **2008**, *77*, 075412.
45. Chen, F.; Klimchitskaya, G.L.; Mohideen, U.; Mostepanenko, V.M. Theory confronts experiment in the Casimir force measurements: Quantification of errors and precision. *Phys. Rev. A* **2004**, *69*, 022117.
46. Klimchitskaya, G.L.; Mohideen, U.; Mostepanenko, V.M. Kramers–Kronig relations for plasma-like permittivities and the Casimir force. *J. Phys. A: Math. Theor.* **2007**, *40*, 339–346.
47. Fosco, C.D.; Lombardo, F.C.; Mazzitelli, F.D. Proximity force approximation for the Casimir energy as a derivative expansion. *Phys. Rev. D* **2011**, *84*, 105031.
48. Bimonte, G.; Emig, T.; Jaffe, R.L.; Kardar, M. Casimir forces beyond the proximity force approximation. *Europhys. Lett.* **2012**, *97*, 50001.
49. Bimonte, G.; Emig, T.; Kardar, M. Material dependence of Casimir force: gradient expansion beyond proximity. *Appl. Phys. Lett.* **2012**, *100*, 074110.
50. Teo, L.P. Material dependence of Casimir interaction between a sphere and a plate: First analytic correction beyond proximity force approximation. *Phys. Rev. D* **2013**, *88*, 045019.
51. Bimonte, G. Going beyond PFA: A precise formula for the sphere-plate Casimir force. *Europhys. Lett.* **2017**, *118*, 20002.
52. Hartmann, M.; Ingold, G.-L.; Maia Neto, P.A. Plasma versus Drude Modeling of the Casimir Force: Beyond the Proximity Force Approximation. *Phys. Rev. Lett.* **2017**, *119*, 043901.
53. Spreng, B.; Hartmann, M.; Henning, V.; Maia Neto, P.A.; Ingold, G.-L. Proximity force approximation and specular reflection: Application of the WKB limit of Mie scattering to the Casimir effect. *Phys. Rev. A* **2018**, *97*, 062504.
54. Hartmann, M.; Ingold, G.-L.; Maia Neto, P.A. Advancing numerics for the Casimir effect to experimentally relevant aspect ratios. *Phys. Scr.* **2018**, *93*, 114003.
55. Maia Neto, P.A.; Lambrecht, A.; Reynaud, S. Casimir effect with rough metallic mirrors. *Phys. Rev. A* **2005**, *72*, 012115.
56. Decca, R.S.; López, D.; Fischbach, E.; Klimchitskaya, G.L.; Krause, D.E.; Mostepanenko, V.M. Tests of new physics from precise measurements of the Casimir pressure between two gold-coated plates. *Phys. Rev. D* **2007**, *75*, 077101.
57. Decca, R.S.; López, D.; Fischbach, E.; Klimchitskaya, G.L.; Krause, D.E.; Mostepanenko, V.M. Novel constraints on light elementary particles and extra-dimensional physics from the Casimir effect. *Eur. Phys. J. C* **2007**, *51*, 963–975.
58. Chang, C.-C.; Banishev, A.A.; Castillo-Garza, R.; Klimchitskaya, G.L.; Mostepanenko, V.M.; Mohideen, U. Gradient of the Casimir force between Au surfaces of a sphere and a plate measured using an atomic force microscope in a frequency-shift technique. *Phys. Rev. B* **2012**, *85*, 165443.
59. Banishev, A.A.; Klimchitskaya, G.L.; Mostepanenko, V.M.; Mohideen, U. Demonstration of the Casimir Force between Ferromagnetic Surfaces of a Ni-Coated Sphere and a Ni-Coated Plate. *Phys. Rev. Lett.* **2013**, *110*, 137401.
60. Banishev, A.A.; Klimchitskaya, G.L.; Mostepanenko, V.M.; Mohideen, U. Casimir interaction between two magnetic metals in comparison with nonmagnetic test bodies. *Phys. Rev. B* **2013**, *88*, 155410.
61. Geyer, B.; Klimchitskaya, G.L.; Mostepanenko, V.M. Thermal Casimir interaction between two magnetodielectric plates. *Phys. Rev. B* **2010**, *81*, 104101.
62. Bimonte, G.; López, D.; Decca, R.S. Isoelectronic determination of the thermal Casimir force. *Phys. Rev. B* **2016**, *93*, 184434.
63. Palik, E.D. (Ed.) *Handbook of Optical Constants of Solids*; Academic Press: New York, NY, USA, 1985.
64. Chen, F.; Klimchitskaya, G.L.; Mostepanenko, V.M.; Mohideen, U. Control of the Casimir force by the modification of dielectric properties with light. *Phys. Rev. B* **2007**, *76*, 035338.
65. Klimchitskaya, G.L.; Mostepanenko, V.M. Conductivity of dielectric and thermal atom-wall interaction. *J. Phys. A: Math. Theor.* **2008**, *41*, 312002.
66. Chang, C.-C.; Banishev, A.A.; Klimchitskaya, G.L.; Mostepanenko, V.M.; Mohideen, U. Reduction of the Casimir Force from Indium Tin Oxide Film by UV Treatment. *Phys. Rev. Lett.* **2011**, *107*, 090403.
67. Banishev, A.A.; Chang, C.-C.; Castillo-Garza, R.; Klimchitskaya, G.L.; Mostepanenko, V.M.; Mohideen, U. Modifying the Casimir force between indium tin oxide film and Au sphere. *Phys. Rev. B* **2012**, *85*, 045436.
68. Bimonte, G. Making precise predictions of the Casimir force between metallic plates via a weighted Kramers–Kronig transform. *Phys. Rev. A* **2011**, *83*, 042109.
69. Klimchitskaya, G.L.; Mostepanenko, V.M.; Svetovoy, V.B. Probing the response of metals to low-frequency s-polarized evanescent waves. *Europhys. Lett.* **2022**, *139*, 66001.
70. Klimchitskaya, G.L.; Mostepanenko, V.M.; Svetovoy, V.B. *Experimentum crucis* for electromagnetic response of metals to evanescent waves and the Casimir puzzle. *Universe* **2022**, *8*, 574.
71. Klimchitskaya, G.L.; Mostepanenko, V.M. An alternative response to the off-shell quantum fluctuations: a step forward in resolution of the Casimir puzzle. *Eur. Phys. J. C* **2020**, *80*, 900.
72. Klimchitskaya, G.L.; Mostepanenko, V.M. Theory-experiment comparison for the Casimir force between metallic test bodies: A spatially nonlocal dielectric response. *Phys. Rev. A* **2022**, *105*, 012805.